Error estimation and adjoint based refinement for an adjoint consistent DG discretisation of the compressible Euler equations

R. Hartmann

Institute of Aerodynamics and Flow Technology,
German Aerospace Center (DLR), Braunschweig, Germany

Institute of Scientific Computing, TU Braunschweig, Germany
E-mail: Ralf.Hartmann@dlr.de

Abstract: Adjoint consistency – in addition to consistency – is the key requirement for discontinuous Galerkin discretisations to be of optimal order in L^2 as well as measured in terms of target functionals. We provide a general framework for analysing adjoint consistency and introduce consistent modifications of target functionals. This framework is then used to derive an adjoint consistent discontinuous Galerkin discretisation of the compressible Euler equations. We demonstrate the effect of adjoint consistency on the accuracy of the flow solution, the smoothness of the discrete adjoint solution and the *a posteriori* error estimation with respect to aerodynamical force coefficients on locally refined meshes.

Keywords: discontinuous Galerkin discretisation; adjoint consistency; compressible Euler equations; continuous adjoint problem; discrete adjoint problem.

Reference to this paper should be made as follows: Hartmann, R. (2007) ‘Error estimation and adjoint based refinement for an adjoint consistent DG discretisation of the compressible Euler equations’, *Int. J. Computing Science and Mathematics*, Vol. 1, Nos. 2/3/4, pp.207–220.

Biographical notes: Ralf Hartmann is Head of a Helmholtz junior research group developing discontinuous Galerkin methods at the Institute of Aerodynamics and Flow Technology at DLR, Braunschweig. He is one of the three authors of the C++ finite element library deal.II, see Bangerth et al. (2005, 2006). He completed his PhD in the numerical methods group of Professor R. Rannacher, University of Heidelberg, in 2002. Since then he has worked on developing discontinuous Galerkin methods towards aerodynamical applications.

1 Introduction

Adjoint consistency, in addition to consistency, is the key requirement for DG discretisations to be of optimal order in L^2 as well as measured in terms of target functional. Furthermore, adjoint consistency is closely related to the smoothness of discrete adjoint solutions. A typical situation is given by the SIPG and NIPG methods, i.e., the symmetric and the asymmetric interior penalty DG discretisation of elliptic PDEs. Whereas adjoint solutions based on the adjoint inconsistent NIPG method are discontinuous between element interfaces, where the jumps in the adjoint solutions even persist as the mesh is refined, see Harriman et al. (2003), the adjoint solutions based on the adjoint consistent SIPG method are essentially continuous, see also Harriman et al. (2004) for an appropriate modification of a flux functional for elliptic PDEs. Furthermore, we refer to the topic of asymptotic adjoint consistency of stabilised finite element methods (Houston et al., 2000). Recently, Lu (2005) and Lu and Darmofal (2006) proposed a specific discretisation of the boundary fluxes and the target functional to recover an adjoint consistent DG discretisation of the compressible Euler equations.

In this paper, we provide a general framework for analysing adjoint consistency of DG discretisations. This framework includes the derivation of the continuous adjoint problems, including continuous adjoint boundary conditions. Furthermore, it includes the derivation of the discrete adjoint problems, the derivation of primal and adjoint residuals and the discussion of the conditions under which residuals vanish for the exact primal and adjoint solutions, respectively. Whereas the standard DG discretisation of the compressible Euler equations, e.g., Bassi and Rebay (1997) and Hartmann and Houston (2002), is not adjoint consistent, we use the outlined framework to derive the adjoint consistent discretisation of the compressible Euler equations originally stated in Lu (2005) and Lu and Darmofal (2006). The proposed framework is generic and particularly useful for deriving adjoint consistent discretisations of more complex non-linear problems. We note that this framework is applied to the analysis and derivation of adjoint consistent DG discretisations of several linear and non-linear problems, including the Poisson's equation and the compressible Navier-Stokes equations in Hartmann (2006a). We also note that the current publication is an extended version of Hartmann (2006b).

In this paper we present numerical experiments demonstrating the effect of adjoint consistency on the accuracy of an inviscid compressible flow around the NACA0012 airfoil. Furthermore, we demonstrate the effect of adjoint consistency on the smoothness of discrete adjoint solutions as well as on the *a posteriori* error estimation with respect to aerodynamical force coefficients on adaptively refined meshes. Further numerical experiments show that due to the smoothness of the discrete adjoint solution the effort of the standard error estimation approach can be significantly reduced. Given a flow solution computed with polynomial degree p, the approach in e.g., Hartmann and Houston (2002, 2006b) computes the discrete adjoint solution with polynomial degree $p + 1$. Here, we show that for the adjoint consistent discretisation, using a patch-wise interpolation to polynomials of degree $p + 1$ of a discrete adjoint solution computed with the same degree p as the flow solution is sufficient for giving reasonable *a posteriori* error estimation results.

2 Consistency and adjoint consistency

On an bounded open domain $\Omega \subset \mathbb{R}^d$ with boundary Γ we consider following non-linear problem

$$N\mathbf{u} = 0 \text{ in } \Omega, \quad B\mathbf{u} = \mathbf{g} \text{ on } \Gamma, \tag{1}$$

where N is a non-linear differential (and Fréchet-differentiable) operator and B is a possibly non-linear boundary operator. Let $J(\cdot)$ be a non-linear target functional

$$J(\mathbf{u}) = \int_\Omega j_\Omega(\mathbf{u})\,\mathrm{d}\mathbf{x} + \int_\Gamma j_\Gamma(\mathbf{u})\,\mathrm{d}s, \tag{2}$$

with Fréchet derivative

$$J'[\mathbf{u}](\mathbf{w}) = \int_\Omega j'_\Omega[\mathbf{u}]\mathbf{w}\,\mathrm{d}\mathbf{x} + \int_\Gamma j'_\Gamma[\mathbf{u}]\mathbf{w}\,\mathrm{d}s,$$

where $j_\Omega(\cdot)$ and $j_\Gamma(\cdot)$ may be non-linear with derivatives j'_Ω and j'_Γ. Here, $'$ denotes the Fréchet derivative and the square bracket $[\cdot]$ denotes the state where the Fréchet derivative is evaluated. Then, the adjoint problem to equation (1) is given by

$$(N'[\mathbf{u}])^*\mathbf{z} = j'_\Omega[\mathbf{u}] \text{ in } \Omega, \quad (B'[\mathbf{u}])^*\mathbf{z} = j'_\Gamma[\mathbf{u}] \text{ on } \Gamma, \tag{3}$$

where $(N'[\mathbf{u}])^*$ and $(B'[\mathbf{u}])^*$ denote the adjoint operators to $N'[\mathbf{u}]$ and $B'[\mathbf{u}]$, respectively. Let Ω be subdivided into shape-regular meshes $\mathcal{T}_h = \{\kappa\}$ consisting of elements κ and let $\mathbf{V}_h$ be a discrete function space on $\mathcal{T}_h$. Finally, let problem (1) be discretised as follows: Find $\mathbf{u}_h \in \mathbf{V}_h$ such that

$$\mathcal{N}(\mathbf{u}_h, \mathbf{v}) = 0 \quad \forall \mathbf{v} \in \mathbf{V}_h, \tag{4}$$

where $\mathcal{N}$ is a semi-linear form. Then, the discretisation (equation (4)) is said to be *consistent* if the solution $\mathbf{u}$ to the primal problem (1) satisfies following equation:

$$\mathcal{N}(\mathbf{u}, \mathbf{v}) = 0 \quad \forall \mathbf{v} \in \mathbf{V}, \tag{5}$$

where $\mathbf{V}$ is an appropriately chosen function space. The discretisation (equation (4)) is said to be *adjoint consistent* if the exact solution $\mathbf{z}$ to the adjoint problem (3) satisfies following equation:

$$\mathcal{N}'[\mathbf{u}](\mathbf{w}, \mathbf{z}) = J'[\mathbf{u}](\mathbf{w}) \quad \forall \mathbf{w} \in \mathbf{V}, \tag{6}$$

where $\mathcal{N}'[\mathbf{u}]$ denotes the Fréchet derivative of $\mathcal{N}$ with respect to its first argument.

In other words, a discretisation is adjoint consistent if the associated discrete adjoint problem is a consistent discretisation of the continuous adjoint problem. Finally, we note, that the definition in equation (6) of adjoint consistency for non-linear problems, see also Lu and Darmofal (2006), generalises the definition of linear adjoint consistency, in that for linear problems and target functionals, it reduces to the definition of linear adjoint consistency as given in e.g., Arnold et al. (2002).

For analysing consistency of a DG discretisation, we rewrite equation (4) in the following primal residual form: Find $\mathbf{u}_h \in \mathbf{V}_h$ such that

$$\sum_{\kappa\in\mathcal{T}_h} \int_\kappa \mathbf{R}(\mathbf{u}_h)\cdot\mathbf{v}\,\mathrm{d}\mathbf{x} + \sum_{\kappa\in\mathcal{T}_h} \int_{\partial\kappa\setminus\Gamma} \mathbf{r}(\mathbf{u}_h)\cdot\mathbf{v}\,\mathrm{d}s + \int_\Gamma \mathbf{r}_\Gamma(\mathbf{u}_h)\cdot\mathbf{v}\,\mathrm{d}s = 0 \quad \forall \mathbf{v} \in \mathbf{V}_h, \tag{7}$$

where $\mathbf{R}(\mathbf{u}_h)$, $\mathbf{r}(\mathbf{u}_h)$ and $\mathbf{r}_\Gamma(\mathbf{u}_h)$ denote the element, interior face and boundary residuals, respectively. According to equation (5), the discretisation is *consistent* if the exact solution $\mathbf{u}$ to equation (1) satisfies

$$\sum_{\kappa\in\mathcal{T}_h}\int_\kappa \mathbf{R}(\mathbf{u})\cdot \mathbf{v}\mathrm{d}\mathbf{x}+\sum_{\kappa\in\mathcal{T}_h}\int_{\partial\kappa\setminus\Gamma}\mathbf{r}(\mathbf{u})\cdot\mathbf{v}\mathrm{d}s+\int_\Gamma \mathbf{r}_\Gamma(\mathbf{u})\cdot\mathbf{v}\mathrm{d}s=0\quad\forall\mathbf{v}\in\mathbf{V}, \tag{8}$$

which holds if **u** satisfies

$$\begin{aligned}&\mathbf{R}(\mathbf{u})=0\quad \text{in } \kappa, \kappa\in\mathcal{T}_h,\\&\mathbf{r}(\mathbf{u})=0\quad \text{on } \partial\kappa\setminus\Gamma, \kappa\in\mathcal{T}_h,\\&\mathbf{r}_\Gamma(\mathbf{u})=0\quad \text{on } \Gamma.\end{aligned} \tag{9}$$

To analyse adjoint consistency, we rewrite the discrete adjoint problem: Find $\mathbf{z}_h \in \mathbf{V}_h$ such that

$$\mathcal{N}'[\mathbf{u}_h](\mathbf{w},\mathbf{z}_h)=J'[\mathbf{u}_h](\mathbf{w})\quad\forall\mathbf{w}\in\mathbf{V}_h, \tag{10}$$

in adjoint residual form: Find $\mathbf{z}_h \in \mathbf{V}_h$ such that

$$\sum_{\kappa\in\mathcal{T}_h}\int_\kappa \mathbf{w}\cdot\mathbf{R}^*(\mathbf{z}_h)\mathrm{d}\mathbf{x}+\sum_{\kappa\in\mathcal{T}_h}\int_{\partial\kappa\setminus\Gamma}\mathbf{w}\cdot\mathbf{r}^*(\mathbf{z}_h)\mathrm{d}s+\int_\Gamma \mathbf{w}\cdot\mathbf{r}_\Gamma^*(\mathbf{z}_h)\mathrm{d}s=0\quad\forall\mathbf{w}\in\mathbf{V}_h, \tag{11}$$

where $\mathbf{R}^*(\mathbf{z}_h)$, $\mathbf{r}^*(\mathbf{z}_h)$ and $\mathbf{r}_\Gamma^*(\mathbf{z}_h)$ denote the element, interior face and boundary adjoint residuals, respectively. According to equation (6), the discretisation (equation (4)) is adjoint consistent if the exact solution **z** to equation (3) satisfies

$$\sum_{\kappa\in\mathcal{T}_h}\int_\kappa \mathbf{w}\cdot\mathbf{R}^*(\mathbf{z})\mathrm{d}\mathbf{x}+\sum_{\kappa\in\mathcal{T}_h}\int_{\partial\kappa\setminus\Gamma}\mathbf{w}\cdot\mathbf{r}^*(\mathbf{z})\mathrm{d}s+\int_\Gamma \mathbf{w}\cdot\mathbf{r}_\Gamma^*(\mathbf{z})\mathrm{d}s=0\quad\forall\mathbf{w}\in\mathbf{V}, \tag{12}$$

which holds if **z** satisfies

$$\begin{aligned}&\mathbf{R}^*(\mathbf{z})=0\quad \text{in } \kappa, \kappa\in\mathcal{T}_h,\\&\mathbf{r}^*(\mathbf{z})=0\quad \text{on } \partial\kappa\setminus\Gamma, \kappa\in\mathcal{T}_h,\\&\mathbf{r}_\Gamma^*(\mathbf{z})=0\quad \text{on } \Gamma.\end{aligned} \tag{13}$$

Given a target functional of the form (equation (2)), we see that $\mathbf{R}^*(\mathbf{z}_h)$ depends on $j_\Omega(\cdot)$, and $\mathbf{r}_\Gamma^*(\mathbf{z}_h)$ depends on $j_\Gamma(\cdot)$. For obtaining adjoint consistent discretisations, it is, in some cases, see e.g., the following section, necessary to modify the target functional as follows

$$\tilde{J}(\mathbf{u}_h)=J(\mathbf{i}(\mathbf{u}_h)), \tag{14}$$

where $i(\cdot)$ is a vector-valued function and will be specified in Section 3. A modification of a target functional is called *consistent* if $\tilde{J}(\mathbf{u})=J(\mathbf{u})$ holds for the exact solution **u** to the primal problem (1). Thereby, the modification in equation (14) is consistent if the exact solution **u** satisfies $\mathbf{i}(\mathbf{u})=\mathbf{u}$. Although the true value of the target functional is unchanged, the computed value $J(\mathbf{u}_h)$ of the target functional is modified, and more importantly, $\tilde{J}'[\mathbf{u}_h]$ differs from $J'[\mathbf{u}_h]$. This modification can be used to recover an adjoint consistent discretisation.

3 The adjoint consistency analysis

In this section we perform the adjoint consistency analysis for the DG discretisation of the compressible Euler equations. To this end, we consider the two-dimensional stationary compressible Euler equations

$$\nabla \cdot \mathcal{F}(\mathbf{u}) = 0 \quad \text{in } \Omega \subset \mathbb{R}^2, \tag{15}$$

subject to various boundary conditions, e.g., slip-wall boundary conditions at solid wall boundaries $\Gamma_w \subset \Gamma = \partial\Omega$, where a vanishing normal velocity

$$B\mathbf{u} = \mathbf{v} \cdot \mathbf{n} = v_1 n_1 + v_2 n_2 = 0 \quad \text{on } \Gamma_W \tag{16}$$

is imposed. In two space-dimensions, the vector of conservative variables $\mathbf{u}$ and the convective fluxes $\mathcal{F}(\mathbf{u}) = (\mathbf{f}_1(\mathbf{u}), \mathbf{f}_2(\mathbf{u}))$ are defined by $\mathbf{u} = (\rho, \rho v_1, \rho v_2, \rho E)^\top$,

$$\mathbf{f}_1(\mathbf{u}) = \begin{bmatrix} \rho v_1 \\ \rho v_1^2 + p \\ \rho v_1 v_2 \\ \rho H v_1 \end{bmatrix} \text{ and } \mathbf{f}_2(\mathbf{u}) = \begin{bmatrix} \rho v_2 \\ \rho v_1 v_2 \\ \rho v_2^2 + p \\ \rho H v_2 \end{bmatrix},$$

where ρ, $\mathbf{v} = (v_1, v_2)^\top$, p and E denote the density, velocity vector, pressure and specific total energy, respectively. Additionally, H is the total enthalpy given by $H = E + (p/\rho) = e + (1/2)\mathbf{v}^2 + (p/\rho)$, where e is the specific static internal energy, and the pressure is determined by the equation of state of an ideal gas $p = (\gamma - 1)\rho e$, where $\gamma = c_p/c_v$ is the ratio of specific heat capacities at constant pressure, c_p, and constant volume, c_v; for dry air, $\gamma = 1.4$.

The most important target quantities in inviscid compressible flows are the pressure induced drag and lift coefficients, c_{dp} and c_{lp}, defined by

$$J(\mathbf{u}) = \int_\Gamma j(\mathbf{u}) \mathrm{d}s = \frac{1}{C_\infty} \int_{\Gamma_W} p\mathbf{n} \cdot \psi \mathrm{d}s, \tag{17}$$

where $j(\mathbf{u}) = (1/C_\infty) p\mathbf{n} \cdot \psi$ on Γ_w and $j(\mathbf{u}) \equiv 0$ elsewhere. Here,

$$C_\infty = (1/2)\gamma p_\infty M_\infty^2 \bar{l} = (1/2)\gamma(|\mathbf{v}_\infty|^2 / c_\infty^2) p_\infty \bar{l} = (1/2)\rho_\infty |\mathbf{v}_\infty|^2 \bar{l},$$

where M denotes the Mach number, c the sound speed defined by $c^2 = \gamma p/\rho$, $\bar{l}$ denotes a reference length, and ψ is given by $\psi_d = (\cos(\alpha), \sin(\alpha))^\top$ or $\psi_l = (-\sin(\alpha), \cos(\alpha))^\top$ for the drag and lift coefficient, respectively. Subscripts $_\infty$, indicate free-stream quantities.

In order to derive the continuous adjoint problem, we multiply the left hand side of equation (15) by $\mathbf{z}$, integrate by parts and linearise about $\mathbf{u}$ to obtain

$$(\nabla \cdot (\mathcal{F}'[\mathbf{u}](\mathbf{w})), \mathbf{z})_\Omega = -(\mathcal{F}'[\mathbf{u}](\mathbf{w}), \nabla \mathbf{z})_\Omega + (\mathbf{n} \cdot \mathcal{F}'[\mathbf{u}](\mathbf{w}), \mathbf{z})_\Gamma,$$

where $\mathcal{F}'[\mathbf{u}]$ denotes the Fréchet derivative of $\mathcal{F}$ with respect to $\mathbf{u}$. Thereby, the variational formulation of the continuous adjoint problem is given by: Find $\mathbf{z}$ such that

$$-(\mathbf{w}, (\mathcal{F}'[\mathbf{u}])^\top \nabla \mathbf{z})_\Omega + (\mathbf{w}, (\mathbf{n} \cdot \mathcal{F}'[\mathbf{u}])^\top \mathbf{z})_\Gamma = J'[\mathbf{u}](\mathbf{w}),$$

for all **w**, and the continuous adjoint solution **z** satisfies following problem in strong form

$$\begin{aligned} -(\mathcal{F}'[\mathbf{u}])^\top \nabla \mathbf{z} = 0 \qquad &\text{in } \Omega, \\ (\mathbf{n}\cdot\mathcal{F}'[\mathbf{u}])^\top \mathbf{z} = j'[\mathbf{u}] \quad &\text{on } \Gamma. \end{aligned} \tag{18}$$

Using $\mathcal{F}(\mathbf{u}) \cdot \mathbf{n} = p(0, n_1, n_2, 0)^\top$ on Γ_W, and the definition of $j(\cdot)$ in equation (17) we obtain

$$p'[\mathbf{u}](0, n_1, n_2, 0) \cdot \mathbf{z} = \frac{1}{C_\infty} p'[\mathbf{u}]\mathbf{n} \cdot \psi \quad \text{on } \Gamma_W,$$

which reduces to the boundary conditions of the adjoint compressible Euler equations,

$$(B'[\mathbf{u}])^* \mathbf{z} = n_1 z_2 + n_2 z_3 = \frac{1}{C_\infty} \mathbf{n} \cdot \psi \quad \text{on } \Gamma_W. \tag{19}$$

We note that, in general, it is unclear whether the primal problems (15) and (16), and the adjoint problems (18) and (19), are well-posed. Therefore, in the subsequent analysis we must assume that these problems are well-posed. Furthermore, we note that the analysis assumes sufficient regularity of the primal and adjoint solutions.

Before introducing the DG discretisation of equation (15) we define the finite element space $\mathbf{V}_h^p$ of discontinuous piecewise vector-valued polynomial functions of degree $p > 0$ by

$$\begin{aligned} \mathbf{V}_h^p = \{\mathbf{v}_h \in [L_2(\Omega)]^4 : \mathbf{v}_h|_\kappa \circ \sigma_\kappa \in [\mathcal{Q}_p(\hat{\kappa})]^4 \quad &\text{if } \hat{\kappa} = \hat{c}, \text{ and} \\ \mathbf{v}_h|_\kappa \circ \sigma_\kappa \in [\mathcal{P}_p(\hat{\kappa})]^4 \quad &\text{if } \hat{\kappa} = \hat{s}; \kappa \in \mathcal{T}_h\}, \end{aligned}$$

where $\mathcal{Q}_p := \text{span}\{\hat{\mathbf{x}}^\alpha : 0 \le \alpha_i \le p, i = 1,2\}$, $\mathcal{P}_p = \text{span}\{\hat{\mathbf{x}}^\alpha : 0 \le |\alpha| \le p\}$, $\hat{c}$ is the unit square and $\hat{s}$ is the unit triangle. On interior edges $e = \partial\kappa \cap \partial\kappa'$ between two adjacent elements κ and κ', by $\mathbf{v}_\kappa^\pm$ ($\mathbf{v}^\pm$ for short) we denote the traces of **v** taken from within the interior of κ and κ', respectively. Furthermore, we define the jump of **u** by $\lfloor \mathbf{u} \rfloor = \mathbf{u}^+ - \mathbf{u}^-$.

Then, the DG discretisation of equation (15) is given by: Find $\mathbf{u}_h \in \mathbf{V}_h^p$ such that

$$\begin{aligned} \mathcal{N}(\mathbf{u}_h, \mathbf{v}) \equiv -\int_\Omega \mathcal{F}(\mathbf{u}_h) : \nabla_h \mathbf{v} \mathrm{d}\mathbf{x} + \sum_{\kappa \in \mathcal{T}_h} \int_{\partial\kappa \setminus \Gamma} \mathcal{H}(\mathbf{u}_h^+, \mathbf{u}_h^-, \mathbf{n}^+)\mathbf{v}^+ \mathrm{d}s \\ + \int_\Gamma \tilde{\mathcal{H}}(\mathbf{u}_h^+, \mathbf{u}_\Gamma(\mathbf{u}_h^+), \mathbf{n}^+)\mathbf{v}^+ \mathrm{d}s = 0, \end{aligned} \tag{20}$$

for all $\mathbf{v} \in \mathbf{V}_h^p$, where $\mathcal{H}$ and $\tilde{\mathcal{H}}$ may be any Lipschitz continuous, consistent and conservative numerical flux functions, see e.g., Hartmann and Houston (2002), approximating the normal flux $\mathbf{n} \cdot \mathcal{F}(\mathbf{u}_h)$. $\mathcal{H}$ takes into account the possible discontinuities of $\mathbf{u}_h$ at element interfaces. On the boundary Γ, $\tilde{\mathcal{H}}$ may depend on the interior trace $\mathbf{u}_h^+$ and a consistent boundary function $\mathbf{u}_\Gamma(\mathbf{u}_h^+)$. We note that $\tilde{\mathcal{H}}$ may be different from $\mathcal{H}$. In fact, we will see below that, depending on the specific choice of $\tilde{\mathcal{H}}$ the DG discretisation (equation (20)) is either adjoint consistent or not.

Using integration by parts we obtain equation (7) where the primal residuals are given by

$$\mathbf{R}(\mathbf{u}_h) = -\nabla\cdot\mathcal{F}(\mathbf{u}_h) \quad \text{in } \kappa, \kappa\in\mathcal{T}_h,$$
$$\mathbf{r}(\mathbf{u}_h) = \mathbf{n}\cdot\mathcal{F}(\mathbf{u}_h^+) - \mathcal{H}(\mathbf{u}_h^+, \mathbf{u}_h^-, \mathbf{n}^+) \quad \text{on } \partial\kappa\setminus\Gamma, \kappa\in\mathcal{T}_h,$$
$$\mathbf{r}_\Gamma(\mathbf{u}_h) = \mathbf{n}\cdot\mathcal{F}(\mathbf{u}_h^+) - \tilde{\mathcal{H}}(\mathbf{u}_h^+, \mathbf{u}_\Gamma(\mathbf{u}_h^+), \mathbf{n}^+) \quad \text{on } \Gamma.$$

Given the consistency of the numerical flux, $\mathcal{H}(\mathbf{w}, \mathbf{w}, \mathbf{n}) = \mathbf{n}\cdot\mathcal{F}(\mathbf{w})$, and the consistency of the boundary function, i.e., $\mathbf{u}_\Gamma(\mathbf{u}) = \mathbf{u}$ for the exact solution $\mathbf{u}$ to equation (15), we find that $\mathbf{u}$ satisfies

$$\mathbf{R}(\mathbf{u}) = 0 \quad \text{in } \kappa, \kappa\in\mathcal{T}_h,$$
$$\mathbf{r}(\mathbf{u}) = 0 \quad \text{on } \partial\kappa\setminus\Gamma, \kappa\in\mathcal{T}_h,$$
$$\mathbf{r}_\Gamma(\mathbf{u}_h) = 0 \quad \text{on } \Gamma.$$

We conclude that equation (20) is a consistent discretisation of equation (15).

Given the target functional $J(\cdot)$ defined in equation (17) with Fréchet derivative, $J'[\mathbf{u}](\cdot)$, the discrete adjoint problem is given by equation (10), where

$$\begin{aligned}\mathcal{N}'[\mathbf{u}_h](\mathbf{w},\mathbf{z}_h) \equiv &-\int_\Omega (\mathcal{F}'[\mathbf{u}_h]\mathbf{w}) : \nabla_h \mathbf{z}_h \mathrm{d}\mathbf{x} \\ &+ \sum_{\kappa\in\mathcal{T}_h} \int_{\partial\kappa\setminus\Gamma} (\mathcal{H}'_{u^+}(\mathbf{u}_h^+,\mathbf{u}_h^-,\mathbf{n}^+)\mathbf{w}^+ + \mathcal{H}'_{u^-}(\mathbf{u}_h^+,\mathbf{u}_h^-,\mathbf{n}^+)\mathbf{w}^-)\mathbf{z}_h^+ \mathrm{d}s \\ &+ \int_\Gamma (\tilde{\mathcal{H}}'_{u^+}(\mathbf{u}_h^+,\mathbf{u}_\Gamma(\mathbf{u}_h^+),\mathbf{n}^+) + \tilde{\mathcal{H}}'_{u^-}(\mathbf{u}_h^+,\mathbf{u}_\Gamma(\mathbf{u}_h^+),\mathbf{n}^+)\mathbf{u}'_\Gamma(\mathbf{u}_h^+))\mathbf{w}^+\mathbf{z}_h^+ \mathrm{d}s.\end{aligned} \tag{21}$$

Here $\mathbf{v}\to\mathcal{H}'_{\mathbf{u}^+}(\mathbf{v}^+,\mathbf{v}^-,\mathbf{n})$ and $\mathbf{v}\to\mathcal{H}'_{\mathbf{u}^-}(\mathbf{v}^+,\mathbf{v}^-,\mathbf{n})$ denote the derivatives of the flux function $\mathcal{H}(\cdot,\cdot,\cdot)$ with respect to its first and second arguments, respectively. As the numerical flux is conservative, $\mathcal{H}(\mathbf{v}, \mathbf{w}, \mathbf{n}) = -\mathcal{H}(\mathbf{w}, \mathbf{v}, -\mathbf{n})$, we conclude

$$\begin{aligned}\mathcal{H}'_{\mathbf{u}^-}(\mathbf{v},\mathbf{w},\mathbf{n}) &= \frac{\partial}{\partial\mathbf{w}}\mathcal{H}(\mathbf{v},\mathbf{w},\mathbf{n}) \\ &= -\frac{\partial}{\partial\mathbf{w}}\mathcal{H}(\mathbf{v},\mathbf{w},-\mathbf{n}) = -\mathcal{H}'_{u^+}(\mathbf{w},\mathbf{v},-\mathbf{n}).\end{aligned}$$

Using this, the discrete adjoint problem (10) is rewritten as follows: Find $\mathbf{z}_h\in\mathbf{V}_h^p$ such that

$$\begin{aligned}&-\int_\Omega (\mathcal{F}'[\mathbf{u}_h]\mathbf{w}) : \nabla_h\mathbf{z}_h\mathrm{d}\mathbf{x} + \sum_{\kappa\in\mathcal{T}_h}\int_{\partial\kappa\setminus\Gamma}\mathcal{H}'_{u^+}(\mathbf{u}_h^+,\mathbf{u}_h^-,\mathbf{n}^+)\mathbf{w}^+\lfloor\mathbf{z}_h\rfloor\mathrm{d}s \\ &\quad + \int_\Gamma(\tilde{\mathcal{H}}'_{u^+}(\mathbf{u}_h^+,\mathbf{u}_\Gamma(\mathbf{u}_h^+),\mathbf{n}^+) + \tilde{\mathcal{H}}'_{u^-}(\mathbf{u}_h^+,\mathbf{u}_\Gamma(\mathbf{u}_h^+),\mathbf{n}^+)\,\mathbf{u}'_\Gamma\,(\mathbf{u}_h^+))\mathbf{w}^+\mathbf{z}_h^+\mathrm{d}s = J'[\mathbf{u}_h](\mathbf{w}),\end{aligned}$$

for all $\mathbf{w}\in\mathbf{V}_h^p$. We see that the discrete adjoint solution $\mathbf{z}_h$ must satisfy following problem

$$-(\mathcal{F}'[\mathbf{u}])^\top\nabla\mathbf{z} = 0 \quad \text{in } \kappa, \kappa\in\mathcal{T}_h, \tag{22}$$

subject to inter-element conditions

$$(\mathcal{H}'_{\mathbf{u}^+}(\mathbf{u}^+,\mathbf{u}^-,\mathbf{n}^+))^\top\lfloor\mathbf{z}\rfloor = 0 \quad \text{on } \partial\kappa\setminus\Gamma, \kappa\in\mathcal{T}_h, \tag{23}$$

and boundary conditions

$$(\tilde{\mathcal{H}}'_{\mathbf{u}^+} + \tilde{\mathcal{H}}'_{\mathbf{u}^-}\mathbf{u}'_\Gamma(\mathbf{u}))^\top \mathbf{z} = j'[\mathbf{u}] \quad \text{on } \Gamma, \tag{24}$$

in a weak sense, where $\tilde{\mathcal{H}}'_{\mathbf{u}^+} := \tilde{\mathcal{H}}'_{\mathbf{u}^+}(\mathbf{u}^+, \mathbf{u}_\Gamma(\mathbf{u}^+), \mathbf{n}^+)$ and $\tilde{\mathcal{H}}'_{\mathbf{u}^-} := \tilde{\mathcal{H}}'_{\mathbf{u}^-}(\mathbf{u}^+, \mathbf{u}_\Gamma(\mathbf{u}^+), \mathbf{n}^+)$.

Comparing the discrete adjoint boundary condition (24) and the continuous adjoint boundary condition in equation (18), we see, that not all choices of $\tilde{\mathcal{H}}$ give rise to an adjoint consistent discretisation. In fact, we require $\tilde{\mathcal{H}}$ to have the following properties: In order to incorporate boundary conditions in the primal discretisation (20), $\tilde{\mathcal{H}}$ must depend on $\mathbf{u}_\Gamma(\mathbf{u}^+)$, hence $\tilde{\mathcal{H}}'_{\mathbf{u}^-} \neq 0$. Furthermore, we require $\tilde{\mathcal{H}}'_{\mathbf{u}^+} = 0$, as otherwise the left hand side of equation (24) involves two summands which is in contrast to equation (18). Finally, we recall that $\tilde{\mathcal{H}}$ is consistent, $\tilde{\mathcal{H}}(\mathbf{v}, \mathbf{v}, \mathbf{n}) = \mathbf{n} \cdot \mathcal{F}(\mathbf{v})$, and conclude that $\tilde{\mathcal{H}}$ is given by $\tilde{\mathcal{H}}(\mathbf{u}_h^+, \mathbf{u}_\Gamma(\mathbf{u}_h^+), \mathbf{n}) = \mathbf{n} \cdot \mathcal{F}(\mathbf{u}_\Gamma(\mathbf{u}_h^+))$. Employing a modified target functional $\tilde{J}(\mathbf{u}_h) = J(\mathbf{i}(\mathbf{u}_h))$, equation (24) yields

$$(\mathbf{n} \cdot (\mathcal{F}'[\mathbf{u}_\Gamma(\mathbf{u}_h^+)])\mathbf{u}'_\Gamma(\mathbf{u}_h^+))^\top \mathbf{z} = j'[\mathbf{i}(\mathbf{u}_h^+)]\mathbf{i}'(\mathbf{u}_h^+). \tag{25}$$

We find the modification $\mathbf{i}(\mathbf{u}_h) = \mathbf{u}_\Gamma(\mathbf{u}_h)$ which is consistent as $\mathbf{i}(\mathbf{u}) = \mathbf{u}_\Gamma(\mathbf{u}) = \mathbf{u}$ holds for the exact solution $\mathbf{u}$. Thereby, equation (25) reduces to

$$(\mathbf{n} \cdot \mathcal{F}'[\mathbf{u}_\Gamma(\mathbf{u}_h^+)])^\top \mathbf{z} = j'[\mathbf{u}_\Gamma(\mathbf{u}_h^+)], \tag{26}$$

which represents a discretisation of the continuous adjoint boundary condition in equation (18). In order to obtain a discretisation of the adjoint boundary condition at solid wall boundaries (equation (19)), we require $B\mathbf{u}_\Gamma(\mathbf{u}^+) = 0$ on Γ_W. This condition is satisfied by

$$\mathbf{u}_\Gamma(\mathbf{u}) = \begin{pmatrix} 1 & 0 & 0 & 0 \\ 0 & 1-n_1^2 & -n_1n_2 & 0 \\ 0 & -n_1n_2 & 1-n_2^2 & 0 \\ 0 & 0 & 0 & 1 \end{pmatrix} \mathbf{u} \quad \text{on } \Gamma_W, \tag{27}$$

which originates from u by subtracting the normal velocity component of $\mathbf{u}$, i.e., $\mathbf{v} = (v_1, v_2)$ is replaced by $\mathbf{v}_\Gamma = \mathbf{v} - (\mathbf{v} \cdot \mathbf{n})\mathbf{n}$ which ensures that the normal velocity component vanishes, $\mathbf{v}_\Gamma \cdot \mathbf{n} = 0$. In summary, let $\mathbf{u}_\Gamma$ be given by equation (27) and $\tilde{\mathcal{H}}$ and $\tilde{J}$ be defined by

$$\tilde{\mathcal{H}}(\mathbf{u}_h^+, \mathbf{u}_\Gamma(\mathbf{u}_h^+), \mathbf{n}) = n \cdot \mathcal{F}_\Gamma(\mathbf{u}_h^+), \quad \tilde{J}(\mathbf{u}_h) = J_\Gamma(\mathbf{u}_h), \tag{28}$$

where $\mathcal{F}_\Gamma(\mathbf{u}_h^+) := \mathcal{F}_\Gamma(\mathbf{u}_\Gamma(\mathbf{u}_h^+))$, $J_\Gamma(\mathbf{u}_h) := J(\mathbf{u}_\Gamma(\mathbf{u}_h))$ and $j_\Gamma(\mathbf{u}_h) := j(\mathbf{u}_\Gamma(\mathbf{u}_h^+))$, then the discrete adjoint problem (10) is given by: Find $\mathbf{z}_h \in \mathbf{V}_h^p$ such that

$$\begin{aligned} -\int_\Omega (\mathcal{F}'[\mathbf{u}_h](\mathbf{w})) : \nabla_h \mathbf{z}_h \mathrm{d}\mathbf{x} + \sum_{\kappa \in \mathcal{T}_h} \int_{\partial\kappa \setminus \Gamma} \mathcal{H}'_{u^+}(\mathbf{u}_h^+, \mathbf{u}_h^-, \mathbf{n}^+)\mathbf{w}^+ \lfloor \mathbf{z}_h \rfloor \mathrm{d}s \\ + \int_\Gamma (\mathbf{n} \cdot \mathcal{F}'_\Gamma[\mathbf{u}_h^+])\mathbf{w}^+ \mathbf{z}_h^+ \mathrm{d}s = J'_\Gamma[\mathbf{u}_h](\mathbf{w}), \end{aligned} \tag{29}$$

for all $\mathbf{w} \in \mathbf{V}_h^p$. Hence, we have the adjoint residual form (equation (11)) where the adjoint residuals are given by

$$\mathbf{R}^*(\mathbf{z}_h) = (\mathcal{F}'[\mathbf{u}_h])^\top \nabla \mathbf{z}_h \quad \text{in } \kappa, \kappa \in \mathcal{T}_h,$$
$$\mathbf{r}^*(\mathbf{z}_h) = -(\mathcal{H}'_{\mathbf{u}^+}(\mathbf{u}^+, \mathbf{u}^-, \mathbf{n}^+))^\top \lfloor \mathbf{z}_h \rfloor \quad \text{on } \partial\kappa \setminus \Gamma, \kappa \in \mathcal{T}_h,$$
$$\mathbf{r}^*_\Gamma(\mathbf{z}_h) = j'_\Gamma[\mathbf{u}] - (\mathbf{n} \cdot \mathcal{F}'_\Gamma[\mathbf{u}])^\top \mathbf{z}_h^+ \quad \text{on } \Gamma.$$

In particular, the discretisation (equation (20)) together with equation (28) is adjoint consistent as the exact solution **z** to the continuous adjoint problem (18) satisfies

$$\mathbf{R}^*(\mathbf{z}) = 0 \quad \text{in } \kappa, \kappa \in \mathcal{T}_h,$$
$$\mathbf{r}^*(\mathbf{z}) = 0 \quad \text{on } \partial\kappa \setminus \Gamma, \kappa \in \mathcal{T}_h, \tag{30}$$
$$\mathbf{r}^*_\Gamma(\mathbf{z}) = 0 \quad \text{on } \Gamma.$$

We note, that the standard DG discretisations of the compressible Euler equations, see e.g., Bassi and Rebay (1997) and Hartmann and Houston (2002, 2006a), among several others, take the same numerical flux function on the boundary Γ as in the interior of the domain, and simply replace $\mathbf{u}_h^-$ in $\mathcal{H}(\mathbf{u}_h^+, \mathbf{u}_h^-, \mathbf{n})$ by the boundary function $\mathbf{u}_\Gamma(\mathbf{u}_h^+)$ resulting in $\tilde{\mathcal{H}}(\mathbf{u}_h^+, \mathbf{u}_\Gamma(\mathbf{u}_h^+), \mathbf{n})$. Furthermore, the definition of $\mathbf{u}_\Gamma$ in e.g., Bassi and Rebay (1997) and Hartmann and Houston (2002) based on $\mathbf{v}_\Gamma = \mathbf{v} - 2(\mathbf{v} \cdot \mathbf{n})\mathbf{n}$ ensures a vanishing average normal velocity, $\tilde{\mathbf{v}} \cdot \mathbf{n} = (1/2)(\mathbf{v} + \mathbf{v}_\Gamma) \cdot \mathbf{n} = 0$. However, $\mathbf{v}_\Gamma \cdot \mathbf{n} = 0$ and $B\mathbf{u}_\Gamma(\mathbf{u}_h^+) = 0$, as required in equation (26), is not satisfied. Thereby, the DG discretisation based on the standard choice of $\tilde{\mathcal{H}}$ and $\mathbf{u}_\Gamma$ is not adjoint consistent. In fact, already the numerical experiments in Hartmann and Houston (2002) indicated large gradients i.e., an irregular adjoint solution near solid wall boundaries. Recently, in Lu (2005) and Lu and Darmofal (2006), it has been demonstrated for an inviscid compressible flow over a bump, that a discretisation based on equation (28) is adjoint consistent and gives rise to a smooth discrete adjoint solution.

4 Numerical experiments

In this section, we will demonstrate the effect on the smoothness of the discrete adjoint solution when employing the adjoint consistent discretisation based on equation (28) in comparison to the standard or classical approach of using

$$\mathcal{H}(\mathbf{u}_h^+, \mathbf{u}_\Gamma(\mathbf{u}_h^+), \mathbf{n}), \quad \text{and} \quad J(\mathbf{u}_h), \tag{31}$$

i.e., of using the same numerical flux on the boundary as in the interior of the domain and evaluating an unmodified functional. Furthermore, we show the effect of the smoothness of the adjoint solution on the *a posteriori* error estimation, see Hartmann and Houston (2002). To this end, we revisit the $M = 0.5$, $\alpha = 0°$ inviscid flow around the NACA0012 airfoil test case considered in Hartmann and Houston (2002). In Figure 1 we compare the flow solutions $\mathbf{u}_h \in \mathbf{V}_h^1$ for the standard and the adjoint consistent DG discretisations and see no visible difference. However, when comparing the adjoint solutions, see Figure 2, we notice that the discrete adjoint solution to the standard DG discretisation is irregular near and upstream of the airfoil. In contrast to that, the adjoint solution to the adjoint consistent discretisation is entirely smooth.

Figure 1 $M = 0.5$; $\alpha = 0°$ inviscid flow around the NACA0012 airfoil: Mach isolines of the (primal) flow solution $\mathbf{u}_h$ to (left) the standard and (right) the adjoint consistent DG discretisation

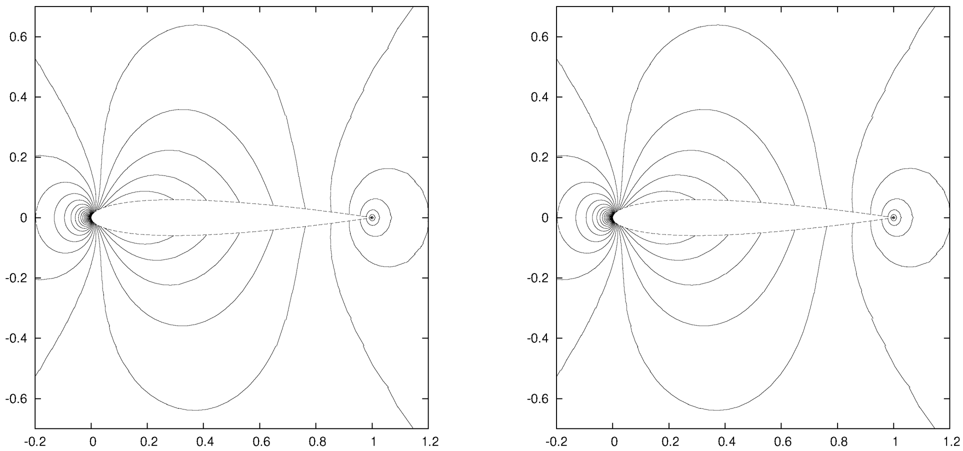

Figure 2 $M = 0.5$; $\alpha = 0°$ inviscid flow around the NACA0012 airfoil: z_1 isolines of the discrete adjoint solution $\mathbf{z}_h$ to (left) the standard and (right) the adjoint consistent DG discretisation

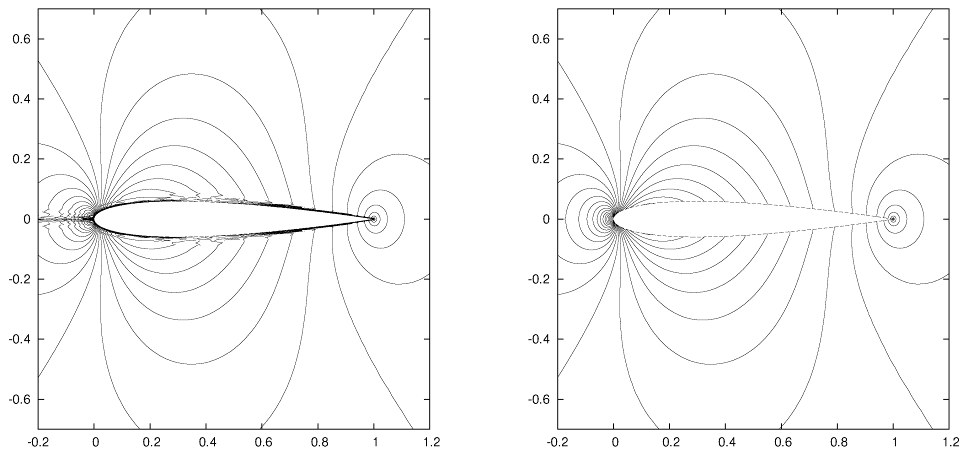

In Tables 1 and 2 we collect the data of a goal-oriented (adjoint-based) adaptive refinement algorithm (Hartmann and Houston, 2002) tailored to the accurate computation of the drag coefficient c_{dp} for the standard and the adjoint consistent DG discretisation, respectively. Here, we show the number of elements and degrees of freedom, the true error $J(\mathbf{u}) - J(\mathbf{u}_h)$ based on the true value $J(\mathbf{u}) = 0$, the estimated error based on the approximate error representation

$$\eta = -\mathcal{N}(\mathbf{u}_h, \mathbf{z}_h) = \sum_{\kappa} \eta_{\kappa} \tag{32}$$

with $\mathbf{z}_h \in \mathbf{V}_h^2$, and the value $\tilde{\eta} = \sum_{\kappa} |\eta_{\kappa}|$ after applying the triangular inequality, together with the corresponding effectivity indices $\theta_1 = \eta / |J(\mathbf{u}) - J(\mathbf{u}_h)|$ and $\theta_2 = \tilde{\eta} / |J(\mathbf{u}) - J(\mathbf{u}_h)|$. Whereas both histories of adaptively refined meshes are almost identical, we see that on all corresponding meshes the adjoint consistent discretisation is, by a factor of about 1.3–2.4, more accurate than the standard DG discretisation. Furthermore, we see that in both cases the error estimation is quite accurate, represented by the fact that θ_1 is close to one. The error estimation for the adjoint consistent discretisation is improved on coarser grids but slightly degraded on finer meshes as compared to the standard DG discretisation. Finally, θ_1 and θ_2 in Table 1 differ significantly, indicating that the standard DG discretisation causes an extensive error cancellation, which is also seen in the irregular discrete adjoint solution. In contrast to that the discrete adjoint solution to the adjoint consistent DG discretisation is smooth, no cancellation effects occur and θ_1 and θ_2 in Table 2 coincide.

Table 1 Error estimation for the standard DG discretisation with $\mathbf{z}_h \in \mathbf{V}_h^2$

# el.	*# DoFs*	$J(\mathbf{u}) - J(\mathbf{u}_h)$	$\eta = \sum_\kappa \eta_\kappa$	θ_1	$\tilde{\eta} = \sum_\kappa \lvert\eta_\kappa\rvert$	θ_2
768	12288	–5.008e–03	–3.279e–03	0.65	7.290e–03	–1.46
1242	19872	–1.783e–03	–1.531e–03	0.86	3.875e–03	–2.17
2061	32976	–5.422e–04	–5.206e–04	0.96	1.382e–03	–2.5
3339	53424	–1.617e–04	–1.632e–04	1.01	4.792e–04	–2.96
5535	88560	–5.060e–05	–5.270e–05	1.04	1.639e–04	–3.24

Table 2 Error estimation for the adjoint consistent DG discretisation with $\mathbf{z}_h \in \mathbf{V}_h^2$

# el.	*# DoFs*	$J(\mathbf{u}) - J(\mathbf{u}_h)$	$\eta = \sum_\kappa \eta_\kappa$	θ_1	$\tilde{\eta} = \sum_\kappa \lvert\eta_\kappa\rvert$	θ_2
768	12288	–3.800e–03	–3.267e–03	0.86	3.270e–03	0.86
1242	19872	–8.833e–04	–8.352e–04	0.95	8.376e–04	0.95
2022	32352	–2.302e–04	–2.139e–04	0.93	2.150e–04	0.93
3327	53232	–8.405e–05	–7.607e–05	0.91	7.658e–05	0.91
5577	89232	–3.754e–05	–3.369e–05	0.90	3.392e–05	0.90

We note that, due to $N(\mathbf{u}_h, \mathbf{v}_h) = 0$ for all $\mathbf{v}_h \in \mathbf{V}_h^p$, see equation (20), the approximate error representation (32) vanishes and is hence, rendered useless if evaluated based on a discrete adjoint solution $\mathbf{z}_h \in \mathbf{V}_h^p$ approximated in the same discrete function space as the flow solution $\mathbf{u}_h \in \mathbf{V}_h^p$. One approach, used in e.g., Hartmann and Houston (2002, 2006b) and in the computations of Tables 1 and 2, is to evaluate the error representation based on $\mathbf{z}_h \in \mathbf{V}_h^{p+1}$, i.e., on a discrete adjoint solution computed with an increased polynomial degree. As the adjoint problem requires the solution of one linear problem in comparison to several linear problems associated with an implicit solution method for the flow problem, this is a viable approach. However, in order to reduce the additional effort associated with the solution of the adjoint problem, in the following we test an alternative approach originally proposed in Becker and Rannacher (1996) of computing the discrete adjoint solution $\mathbf{z}_h \in \mathbf{V}_h^1$ with the same polynomial degree as the flow solution and using a patch-wise interpolation to $\mathbf{V}_{2h}^2$. Here, using a patch we denote the aggregation of e.g., four quadrilateral elements. Typically, in a hierarchically refined mesh, a 'mother' element is split into four 'child' elements which together form a patch. On this patch the discrete function represented by a discontinuous piecewise polynomial of degree p, in fact by four polynomials of degree p, is then interpolated to *one* polynomial of degree $p+1$ on that patch.

In Tables 3 and 4 we collect the data of the goal-oriented adaptive refinement algorithm analogous to Tables 1 and 2 but now based on the patch-wise interpolation of $\mathbf{z}_h \in \mathbf{V}_h^1$ to $\mathbf{V}_{2h}^2$ instead of $\mathbf{z}_h \in \mathbf{V}_h^2$. First, we note that the histories of the local mesh refinement in Tables 3 and 4 are quite similar to the histories in Tables 1 and 2. From this we see that the quality of the adjoint based indicators and resulting adaptive mesh refinement is not significantly decreased when evaluated with $\mathbf{z}_h \in \mathbf{V}_{2h}^2$ as compared to the more costly approach of computing $\mathbf{z}_h \in \mathbf{V}_h^2$. However, for the standard DG discretisation in Table 3 the accuracy of the error estimation is significantly reduced represented by the fact, that the effectivity indices θ_1 vary between 0.25 and 0.71. In contrast to that the indices θ_1 for the adjoint consistent DG discretisation in Table 4 are, except for the coarsest mesh, constant (close to 2/3), showing that the error estimation has the same behaviour under mesh refinement as the true error. This difference is attributed to the fact that the patch-wise interpolated approximation of the adjoint solution is significantly more accurate for the adjoint consistent discretisation where the discrete adjoint solution is smooth than for the standard discretisation with irregular discrete adjoint solutions.

Table 3 Error estimation for the standard DG discretisation with $\mathbf{z}_h \in \mathbf{V}_h^1$ patch-wise interpolated to $\mathbf{V}_{2h}^2$

# el.	*# DoFs*	$J(\mathbf{u})-J(\mathbf{u}_h)$	$\eta=\sum_\kappa \eta_\kappa$	θ_1	$\tilde{\eta}=\sum_\kappa \lvert\eta_\kappa\rvert$	θ_2
768	12288	–5.007e–03	–1.244e–03	0.25	2.528e–03	–0.50
1254	20064	–1.788e–03	–5.668e–04	0.32	1.187e–03	–0.66
2037	32592	–5.567e–04	–2.095e–04	0.38	4.544e–04	–0.82
3351	53616	–1.596e–04	–8.273e–05	0.52	1.656e–04	–1.04
5448	87168	–4.840e–05	–3.451e–05	0.71	6.455e–05	–1.33

Table 4 Error estimation for the adjoint consistent DG discretisation with $\mathbf{z}_h \in \mathbf{V}_h^1$ patch-wise interpolated to $\mathbf{V}_{2h}^2$

# el.	*# DoFs*	$J(\mathbf{u})-J(\mathbf{u}_h)$	$\eta=\sum_\kappa \eta_\kappa$	θ_1	$\tilde{\eta}=\sum_\kappa \lvert\eta_\kappa\rvert$	θ_2
768	12288	–3.799e–03	–1.666e–03	0.44	1.673e–03	–0.44
1248	19968	–8.928e–04	–5.570e–04	0.62	5.599e–04	–0.63
2010	32160	–2.451e–04	–1.512e–04	0.62	1.538e–04	–0.63
3288	52608	–9.020e–05	–5.856e–05	0.65	5.939e–05	–0.66
5337	85392	–4.035e–05	–2.862e–05	0.71	2.878e–05	–0.71

5 Concluding remarks

In this paper, we have provided a general framework for analysing the adjoint consistency property of DG discretisations, introduced consistent modifications of target functional, and derived an adjoint consistent DG discretisation for the compressible Euler equations originally proposed in Lu (2005) and Lu and Darmofal (2006). This included the analysis of the continuous adjoint equations and the adjoint boundary conditions of the compressible Euler equations as well as the discrete adjoint equations and the discretisation of boundary conditions and target functionals.

Numerical experiments have demonstrated that the discrete flow solutions are visibly indistinguishable for the adjoint consistent compared to a standard (i.e., adjoint inconsistent) discretisation, but there is a clear difference in the discrete adjoint solutions: While the discrete adjoint solution to the standard discretisation is irregular near and upstream of the airfoil, the discrete adjoint solution to the adjoint consistent discretisation is entirely smooth. In fact, the discrete adjoint solution for an adjoint consistent discretisation is a consistent discretisation of the continuous adjoint solution and thus inherits the smoothness properties of the continuous adjoint solution.

Further numerical experiments have demonstrated the effect of adjoint consistency on the *a posteriori* error estimation on locally refined meshes. While large error cancellation occurs for the standard discretisation due to the irregular and oscillating discrete adjoint solution near the airfoil, there is virtually no error cancellation for the adjoint consistent discretisation which again indicates an entirely smooth discrete adjoint solution. Furthermore, drag coefficients computed based on the adjoint consistent discretisation were by a factor of about two more accurate than based on the standard discretisation.

Finally, we have tested an alternative approach of *a posteriori* error estimation based on a patch-wise interpolated discrete adjoint solution computed with the same polynomial degree as the flow solution. Whereas this approach yields a poor error estimation for the standard DG discretisation it reproduces the behaviour of the exact error of the adjoint consistent discretisation. Thus, in addition to accuracy improvements of the flow solution already mentioned, adjoint consistent discretisations have the potential to significantly decrease the additional amount of work associated with solving discrete adjoint problems required for error estimation and adjoint based refinement.

Future research will be dedicated to the adjoint consistency analysis of DG discretisations of more complex non-linear problems, see e.g., Hartmann (2006a) for the adjoint consistency analysis of the interior penalty DG discretisation of the compressible Navier-Stokes equations (Hartmann and Houston, 2006a).

Acknowledgements

All computations have been performed with the DG flow solver `PADGE` which is based on the C++ finite element library `deal.II`, (Bangerth et al., 2005, 2006). This work has been supported by the President's Initiative and Networking Fund of the Helmholtz Association of German Research Centres.

References

Arnold, D., Brezzi, F., Cockburn, B. and Marini, D. (2002) 'Unified analysis of discontinuous Galerkin methods for elliptic problems', *SIAM J. Numer. Anal.*, Vol. 39, No. 5, pp.1749–1779.

Bangerth, W., Hartmann, R. and Kanschat, G. (2005) deal.II, *Differential Equations Analysis Library*, *Technical Reference*, 5.2 ed., September, First ed. 1999, http://www.dealii.org/.

Bangerth, W., Hartmann, R. and Kanschat, G. (2006) deal.ii, 'A general purpose object oriented finite element library', *ACM Transactions on Mathematical Software*, Vol. 33, No. 4, To appear, Available as Technical Report ISC06-02-MATH, Texas A&M University, http://www.isc.tamu.edu/publications-reports/tr/0602.pdf.

Bassi, F. and Rebay, S. (1997) 'High-order accurate discontinuous finite element solution of the 2d Euler equations', *J. Comp. Phys.*, Vol. 138, pp.251–285.

Becker, R. and Rannacher, R. (1996) 'A feed-back approach to error control in finite element methods: basic analysis and examples', *East–West J. Numer. Math.*, Vol. 4, pp.237–264.

Harriman, K., Houston, P., Senior, B. and Süli, E. (2003) 'hp–Version discontinuous Galerkin methods with interior penalty for partial differential equations with nonnegative characteristic form', *Recent Advances in Scientific Computing and Partial Differential Equations*, AMS, Vol. 330 of Contemporary Mathematics, pp.89–119.

Harriman, K., Gavaghan, D. and Süli, E. (2004) *The Importance of Adjoint Consistency in the Approximation of Linear Functionals using the Discontinuous Galerkin Finite Element Method*, Oxford University Computing Laboratory, Technical Report, ftp://ftp.comlab.ox.ac.uk/pub/Documents/techreports/NA-04-18.ps.gz.

Hartmann, R. (2006a) 'Adjoint consistency analysis of discontinuous Galerkin discretizations', *SIAM J. Numer. Anal.*, In review.

Hartmann, R. (2006b) 'Derivation of an adjoint consistent discontinuous Galerkin discretization of the compressible Euler equations', in Lube, G. and Rapin, G. (Eds.): *Proceedings of the BAIL* 2006 *Conference*, ISBN: 3-00-019600-5, See also http://www.num.math.uni-goettingen.de/bail.

Hartmann, R. and Houston, P. (2002) 'Adaptive discontinuous Galerkin finite element methods for the compressible Euler equations', *J. Comp. Phys.*, Vol. 183, pp.508–532.

Hartmann, R. and Houston, P. (2006a) 'Symmetric interior penalty DG methods for the compressible Navier–Stokes equations I: method formulation', *Int. J. Num. Anal. Model.*, Vol. 3, No. 1, pp.1–20.

Hartmann, R. and Houston, P. (2006b) 'Symmetric interior penalty DG methods for the compressible Navier–Stokes equations II: goal–oriented a posteriori error estimation', *Int. J. Num. Anal. Model.*, Vol. 3, No. 2, pp.141–162.

Houston, P., Rannacher, R. and Süli, E. (2000) 'A posteriori error analysis for stabilised finite element approximations of transport problems', *Comput. Meth. Appl. Mech. Engrg.*, Vol. 190, Nos. 11–12, pp.1483–1508.

Lu, J. (2005) *An a posteriori Error Control Framework for Adaptive Precision Optimization using Discontinuous Galerkin Finite Element Method*, PhD Thesis, MIT, http://raphael.mit.edu/LuPhD_Thesis.pdf.

Lu, J. and Darmofal, D.L. (2006) 'Dual-consistency analysis and error estimation for discontinuous Galerkin discretization: application to first-order conservation laws', *IMA Journal of Numerical Analysis*, Submitted.